Impact of directionality on the extreme wave occurrence in a discrete random wave system

Takuji Waseda
Dept. Environmental and Ocean Engineering, University of Tokyo

1. Introduction

A number of marine accidents are possibly caused by encounters with the freak waves in the ocean. Numerous researches have therefore been conducted to understand, observe and predict the freak waves in the ocean, particularly in the last 10 years or so. Up until now, however, there is no monitoring system in operation that can detect the sporadic extreme events in the vast ocean. On the other hand, third generation wave models have advanced and are now in operation in various countries and institutions providing global and local wave forecasts. It is therefore practical to utilize numerical wave forecast products to predict freak wave occurrence in the ocean.

The only practical suggestion made so far on the utilization of the wave forecast model to predict freak wave is the introduction of the Benjamin-Feir Index by Janssen (2003). The underlying principle is the near resonance interaction of waves that is inherent in the weakly nonlinear gravity wave system (Zakharov 1967). Janssen has shown by use of the Zakharov equation that the magnitude of the kurtosis can be parameterized by the ratio of wave steepness and spectral bandwidth. Because the simplest case of the non-resonant interaction was first discovered by Benjamin & Feir (1967) in their study of an unstable Stokes wave, the parameter was named the Benjamin-Feir index. The correspondence of the BFI to the extreme wave statistics was first verified experimentally by Onorato et al. (2004) where they have observed the evolution of a uni-directional random wave with JONSWAP type wave spectrum. Extreme wave statistics was controlled by changing the peakedness of the spectrum, effectively changing the frequency bandwidth or the BFI. Such discovery is a great step in understanding the freak wave generation mechanism, however, as the same authors (Onorato et al. 2002), and Soquet-Juglard et al. (2005) have shown numerically, the introduction of directionality of the wave spectrum significantly reduces the extreme wave occurrence. For this reason, there has been a debate whether near-resonance interaction or the bound-wave generation enhancing the extreme wave amplitude in a random Gaussian sea is responsible for the extreme wave generation in the open ocean. (Dysthe et al. 2004)

In this study we extend the experimental work of Onorato et al. (2004) to include directionality of the JONSWAP type spectrum. The result is rather striking that the occurrence of extreme event significantly reduces as the directionality broadens. Preliminary analysis of a systematic experiment varying the directionality and the spectral bandwidth will be introduced in section 3, following the description of the wave tank in section 2. In section 4, the influence of discreteness of the wave system (that is inevitable in both tank and numerical experiments), will be addressed solving the Zakharov equation numerically. Conclusions follow.

2. Tank Experiment

Experiment was conducted at a 50m long, 10 m wide, and 5 m deep wave tank of the Institute of Industrial Science, University of Tokyo (Kinoshita laboratory/Rheem laboratory). The tank is equipped with a segmented plunger type directional wave maker (32 plungers) digitally controlled by arbitrary wave forms. The directional wave was generated using single summation method which assigns single direction for each frequency component (1024 frequencies were used). This method assures ergodicity (i.e. statistics does not depend on the location) and is suitable when the number of sensors is limited (10 wave wires used in this

study) since the wave guide effect of a narrow wave channel is minimized. The frequency spectrum of the JONSWAP type

$$S(f) = \alpha g^2 (2\pi)^{-4} f^{-5} \exp\left\{-\frac{5}{4}\left(\frac{f}{f_p}\right)^{-4}\right\} \gamma^{\exp\left\{-\frac{(f-f_p)^2}{2\sigma^2 f^2 p}\right\}}, \quad (1)$$

is discretized into 1024 components at irregular intervals conserving wave energy for each frequency bin. Then the direction for each wave components are selected randomly from a Mitsuyasu-type directional spreading function,

$$G(\theta) = G_n \cos^n(\theta). \quad (2)$$

The wave signal is constructed as a linear superposition of 1024 waves with random initial phases e_n.

$$\begin{cases} \eta(x,y,t) = \sum_{n=1}^{n=1024} a_n \cos(\omega_n t - \mathbf{k_n} \cdot \mathbf{x} + e_n) \\ a_n = \sqrt{2S(\omega_n)\Delta\omega} \end{cases} \quad (3)$$

The control parameters in this study were α, γ and n, that are closely related to the significant wave height, the frequency bandwidth, and the directional spread respectively. The wavelength at the spectral peak f_p is 1 meter so the tank length is approximately 50 wavelengths. The array of wave wires were arranged at 5 m intervals from 5 to 40 m from the wave maker, 2.6 m away from the side wall; two additional wave wires were arranged at 20 m fetch at 3.8 and 5 meters away from the side wall as well.

Two sets of significant wave heights were selected in this study, the first set corresponds to wave steepness 0.184 ($H_{1/3} = 5.86$ cm) and the second set to wave steepness 0.13 ($H_{1/3} = 4.15$ cm). The latter value is more realistic for the Ocean and so we have studied most extensively this case varying parameters γ and n. The peakedness factor according to fetch laws in the ocean is γ=3.0 for steepness 0.13. Thus, we have conducted a sensitivity study for cases γ=1.0, 3.0 and 30.0 for steepness 0.13. The directional spread is controlled by n and the selected values ranging from n=1 to 125 correspond to 120 to 14 degrees spread angle containing half the total wave energy. Note that the BFI derived as

$$\begin{cases} \delta f^2 = \dfrac{\int f^2 S(f) df}{m_0} - f_p{}^2 \\ BFI = \dfrac{\sqrt{2}\varepsilon}{2\delta f / f_p} \end{cases} \quad (4)$$

ranged between 0.226 and 1.128 and does not depend on the directional spread. Typical frequency spectrum and the directional spreading functions are shown in figure 1.

Finally, for most experimental conditions, breaking waves were observed, but its intensity reduced as the directional spread increased. The analyses of the impact of wave breaking on the wave evolution is underway but will not be presented here. We consider that the effect of breaking wave is essential in understanding the wave evolution, in accordance to the earlier suggestion by Tulin and Waseda (1999).

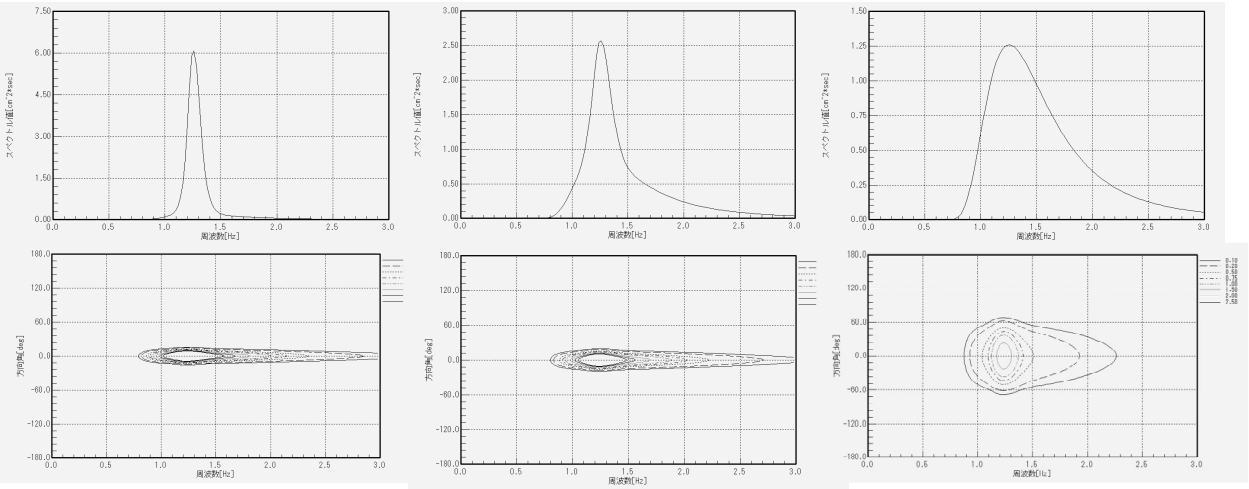

Figure 1 Top row from left to right: JONSWAP type frequency spectrum with γ=30, 3 and 1; bottom row from left to right: directional spectrum with n=125, 75 and 3 for γ=3

3. Results of the tank experiment

For each case, an hour long wave records were taken by 10 wave wires in the tank. Although a longer record is desirable we consider that they provide sufficient accuracy in estimating the extreme wave statistics since each time series contains more than 4000 waves. We first present in figure 2 the fetch evolution of the kurtosis of a uni-directional case (γ=3.0, ε=3.0, BFI=0.3152). Similar to the earlier experimental study by Onorato et al. (2004), the kurtosis initially increases but tends to reduce to a lower value at longer fetches. Vigorous breakers are observed to form in a wave group resembling the Benjamin-Feir instability wave train. There is a spread of kurtosis at 20 m fetch where 3 wave wires were located at different distance from the sidewall (2, 4 and 5 m). The discrepancy is most likely due to the three dimensionality of the breaker as a result of type II instability that kicks in when wave amplitude increases (Melville 1982). Therefore, the variability seen at fetch 20 m is inherent in the experiment including breaking wave. In the rest of the study the kurtosis for each case will be given as an average of those from wave wires at fetches 15 m to 40 m. The mean of the kurtosis is close to 3.6 (with standard deviation less than 0.2) much larger than the linear Gaussian wave system. As Onorato et al. (2005) have shown from the Zakharov equation, the kurtosis can be expressed as a summation of linear Gaussian component, the correction term due to near-resonance interaction (Benjamin-Feir instability of free waves) and the correction due to the distortion of the wave shape (Stokes correction by bound waves)

$$\left\langle \eta^4 \right\rangle = 3\left\langle \eta^2 \right\rangle^2 + \text{H.O.T.(free wave)} + \text{H.O.T.(bound wave)}. \qquad (5)$$

We consider that determination of the relative magnitude of the higher order terms (H.O.T.s) is important but will leave the analyses for future study.

We investigate now the extreme wave statistics from the experiment. The exceedance probability of the wave height is displayed in Figure 3 for the uni-directional case. The distribution of waves below 1.5 or so times the significant wave height Hs seems to fit quite well to the Rayleigh distribution shown as a solid line. The tail of the distribution gradually increases at larger fetch and at fetches 20 and 25 m the tail of the observed distribution is remarkably larger than the Rayleigh distribution. Further down the tank, the tail seems to reduce again and the distribution approaches the Rayleigh distribution. Such tendency seems consistent with the evolution of the kurtosis shown earlier in Figure 2, and also the earlier result by Onorato et al. (2004).

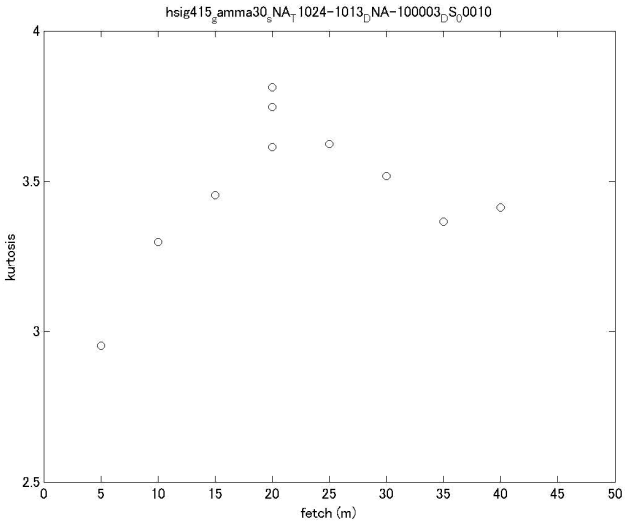

Figure 2 Evolution of kurtosis with fetch for uni-directional JONSWAP spectrum with γ=3.0, ε=3.0, BFI=0.3152

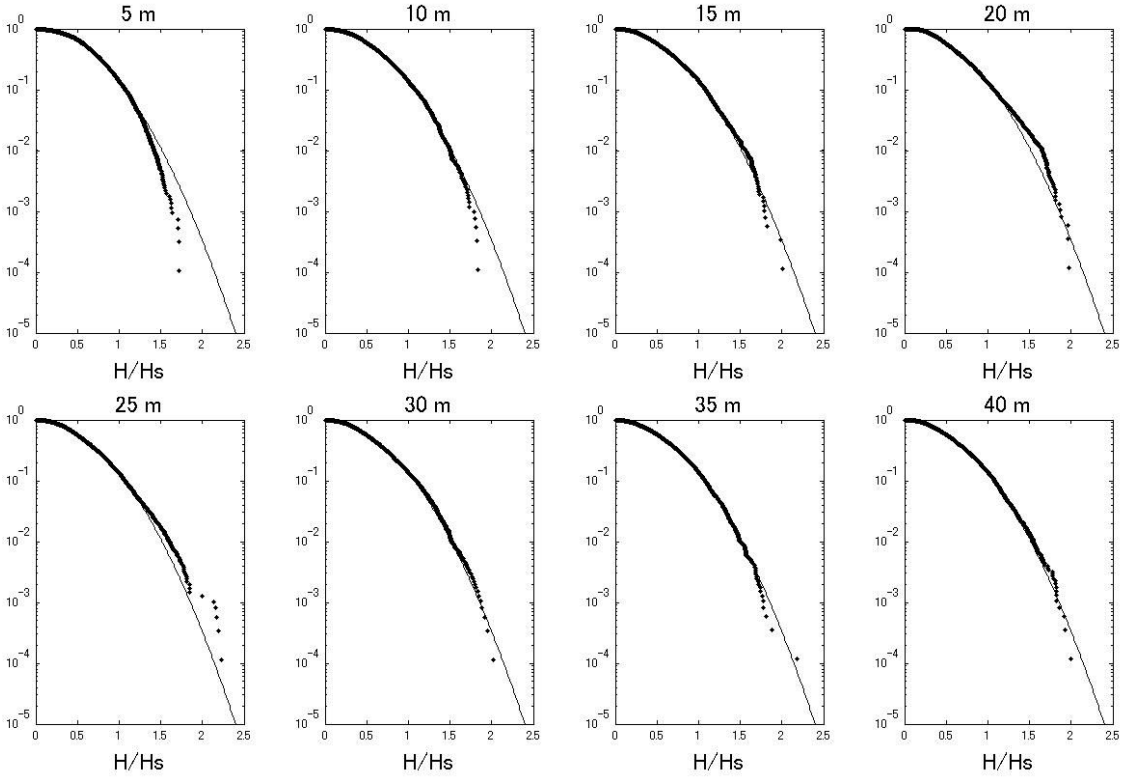

Figure 3 Exceedance probability of the uni-directional JONSWAP spectrum with γ=3.0, ε=3.0, BFI=0.3152, dots: experiment, line: Rayleigh distribution.

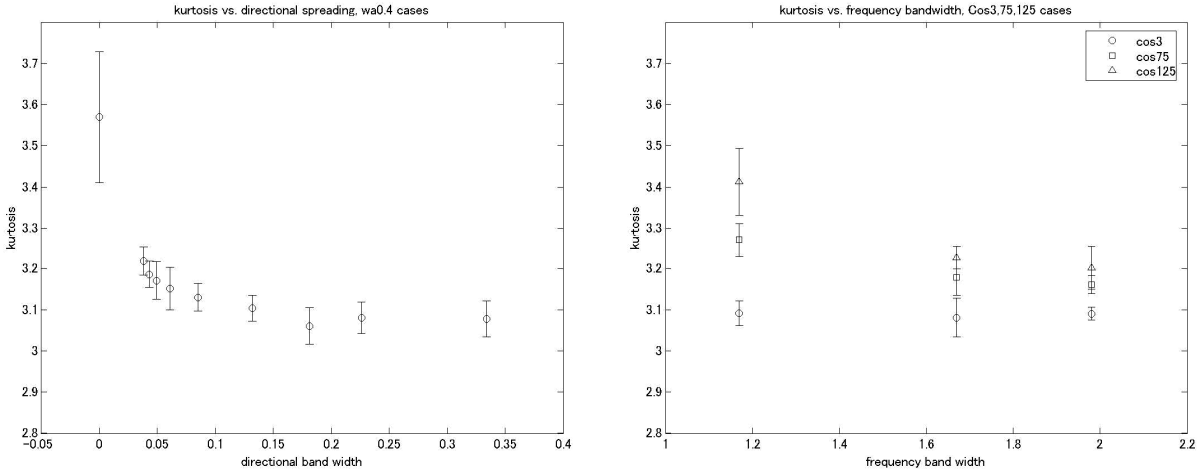

Figure 4 Left: Kurtosis plotted against directional band width for γ=3.0, ε=3.0, BFI=0.3152; Right: Kurtosis plotted against frequency bandwidth (γ=30.0, 3.0 and 1.0 from left to right) for n=3 (circle), n=75 (square) and n=125 (triangle). The error bar is one standard deviation.

The experiment was extended to include directionality. The random wave was generated for directional spectrum defined as (1) and (2) with various parameter values. In Figure 4, the dependences of the kurtosis on directional spreading (left figure) and on the frequency bandwidth (right figure) are summarized. In both figures, the mean value and the standard deviation of the kurtosis are obtained by averaging the estimation from wave records at fetches 15 m and larger. Therefore, the spatial variation of the kurtosis is averaged in this analysis. In the left figure, the frequency spectrum (1) is fixed with γ=3.0, ε=3.0, BFI=0.3152, but the directional spreading was altered from n=1 to 125 in (2). The parameters n=1 to 125 correspond to 120 degrees to 14 degrees spread angle containing half the total energy (Table). As the directional bandwidth increases, the kurtosis drops rapidly (see left figure). At 14 degrees spread angle (n=125), the kurtosis has already dropped to around 3.2, which is about 0.4 reduction from the uni-directional case. Then the kurtosis gradually decreases and at n=5 the value of the kurtosis equilibrate to around 3.1. This is a striking result because all these cases have the same BFI. In other words, the kurtosis can take any values between 3.6 and 3.1 for a given BFI if the directionality is altered. In the open ocean, directional spread of 14 degrees is extremely narrow. Perhaps a realistic spreading is around 30 degrees (directional bandwidth 0.085) or broader, so the expected magnitude of the kurtosis is less than 3.2, much smaller than the uni-directional case.

Does this mean that BFI is an unimportant parameter? For a given directionality, the kurtosis decreases as the frequency bandwidth broadens (or BFI decreases, see Figure 4 right). The rate of decrease, however, depends strongly on the directional spreading; for narrow directional spread, the kurtosis reduces rapidly (triangle) whereas for broad directional spread, the kurtosis is nearly constant (circle) for any frequency bandwidth (or BFI). This result suggests that BFI is a relevant parameter only if the directional spreading is extremely narrow. A value of n=125 (or 14 degrees spread) is unrealistic for wind generated waves in the ocean. Thus, we understand that BFI is a parameter relevant for extremely narrow wave spectrum such as a swell (n=75, square in Figure 4 right).

Table: Exponent n of the Mitsuyasu-type spreading and the directional band width w: $2w\pi$ will give the spreading angle containing half the total energy

n	1	3	5	10	25	50	75	100	125
w	0.334	0.226	0.1817	0.132	0.085	0.061	0.0495	0.0429	0.0384

Finally, Figure 5 summarizes the exceedence probability for different directional spreading (n=125, 75, 3) and frequency bandwidth (γ=30.0, 3.0, 1.0). As one move towards the upper-left corner, the spectrum becomes narrower and so the deviation of the distribution from the Rayleigh distribution becomes large. On the other hand, as one move towards the lower-right corner, the spectrum becomes broader and the distribution tends to fit better to the Rayleigh distribution. And in the broadest case (γ=1, i.e. fully mature Pierson-Moskovitz spectrum) the distribution is over-estimated by the Rayleigh distribution, consistent with the observation in the North Sea by Forristall (1978). The fact that the distribution did not deviate from Rayleigh as much as expected is not a proof that the non-resonant interaction is absent. More study is needed to fully understand the wave evolution in the tank and how that relates to the directional ocean wave system.

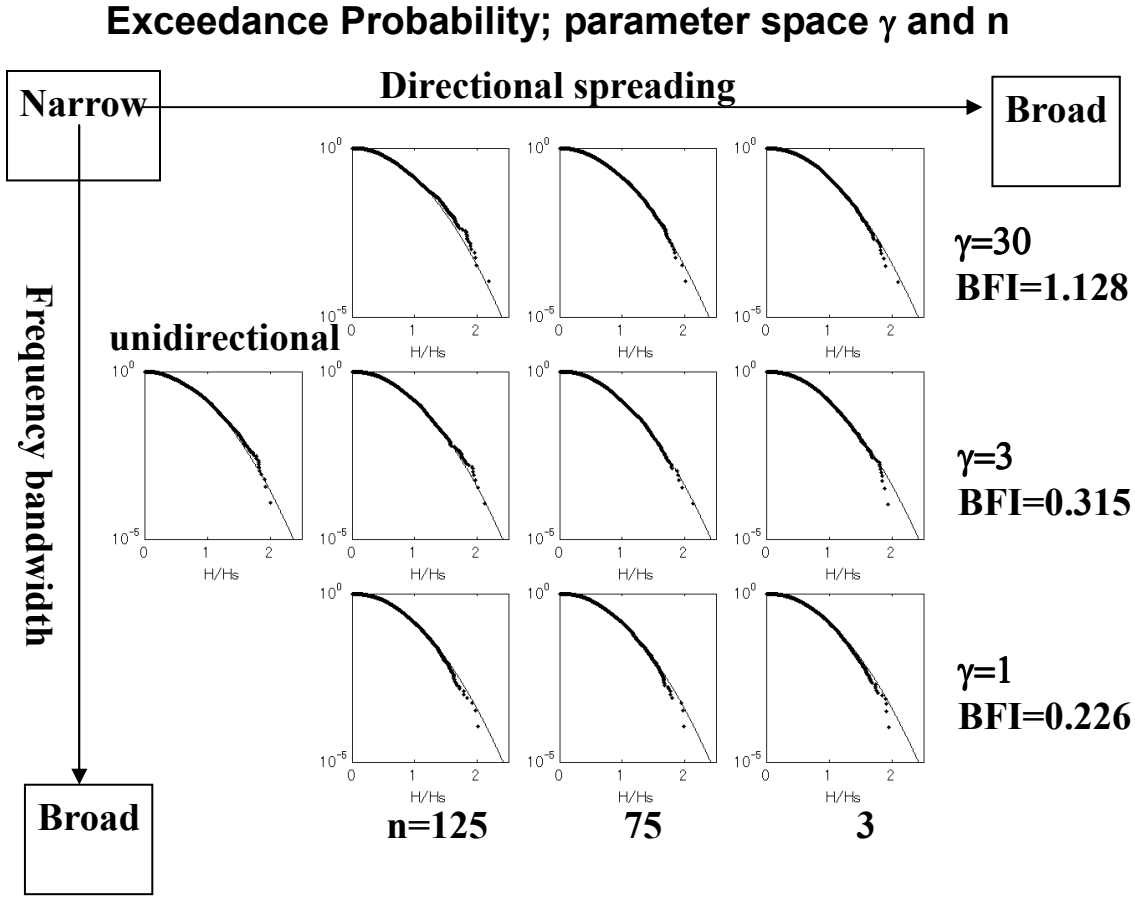

Figure 5 Exceedence probabilities of the selected cases showing dependency on the directional spreading and frequency bandwidth. The wave height distributions are from 40 m fetch.

4. Evolution of discrete wave system, a numerical study

A concern with every tank experiment as well as numerical experiment is the discreteness of the wave system. The plunger motion signal is generated following (1) and (2) but for a discrete system. Other numerical studies conducted in the past typically are solved in a periodic domain and therefore are discrete in wave number space. The solution of course should asymptote to a continuous wave system, as the degree of freedom increases, but rather slowly. In this section we investigate how the evolution of a uni-directional random wave system is altered when the degree of discretization is changed.

The basis of this study is the Zakharov's equation or its modified form by Krasitskii (1994). The so-called 4-wave reduced equation for gravity waves

$$i\frac{\partial B(k_0)}{\partial t} = \int \widetilde{V}^{(2)}_{0,1,2,3} B(k_1)^* B(k_2) B(k_3) \exp\left[i\Delta_{0+1-2-3}t\right]\delta_{0+1-2-3}dk_{123}$$
$$\sigma_0 + \sigma_1 - \sigma_2 - \sigma_2 = \Delta_{0+1-2-3};\quad \delta_{0+1-2-3} = \delta(k_0 + k_1 - k_2 - k_3) \tag{6}$$

is solved numerically in a discrete form $B(k_0,t) = B_0(t)\delta(k-k_0)$:

$$i\frac{dB_0}{dt} = \sum_{\mathbf{k}_0+\mathbf{k}_1=\mathbf{k}_2+\mathbf{k}_3} \widetilde{V}^{(2)}_{0,1,2,3} \exp\left(i\Delta_{0+1-2-3}t\right) B_1^* B_2 B_3$$
$$\sigma_0 + \sigma_1 - \sigma_2 - \sigma_2 = \Delta_{0+1-2-3} \tag{7}$$

Here B_0 is the canonical variable and the physical quantities can be derived in two steps, first by conducting the canonical transformation (actually in a discrete form),

$$\begin{cases} b(k,t) = B(k,t)\exp[-i\omega(k)t] \\ a_0 = b_0 + \int A^{(1)}_{0,1,2} b_1 b_2 \delta_{0-1-2}dk_{12} + \int A^{(2)}_{0,1,2} b_1^* b_2 \delta_{0+1-2}dk_{12} \\ \quad + \int A^{(3)}_{0,1,2} b_1^* b_2^* \delta_{0+1+2}dk_{12} + \int B^{(1)}_{0,1,2,3} b_1 b_2 b_3 \delta_{0-1-2-3}dk_{123} \\ \quad + \int B^{(2)}_{0,1,2,3} b_1^* b_2 b_3 \delta_{0+1-2-3}dk_{123} + \int B^{(3)}_{0,1,2,3} b_1^* b_2^* b_3 \delta_{0+1+2-3}dk_{123} \\ \quad + \int B^{(4)}_{0,1,2,3} b_1^* b_2^* b_3^* \delta_{0+1+2+3}dk_{123} \end{cases} \tag{8}$$

and, next deriving the actual physical variables,

$$\begin{cases} \zeta(k) = M(k)[a(k) + a^*(-k)] \\ \psi(k) = -i\,N(k)[a(k) - a^*(-k)] \\ M(k) = \left[\dfrac{q(k)}{2\omega(k)}\right]^{1/2} \\ N(k) = \left[\dfrac{\omega(k)}{2q(k)}\right]^{1/2} \end{cases} \tag{9}$$

Solving (7) for a discrete random wave system numerically will produce higher order terms related only to the free waves in (5) and by using (8) the bound wave effect will take place. We will not show the relative significance of each term but is possible in the current numerical scheme implemented. We will solve equations (6) to (9) numerically for a uni-directional wave system for a given spectral shape (Gaussian spectrum, randomly initialized) but with different discretization level,

$$W_{oi} = \frac{BFI}{2\sqrt{\pi}} \exp\left(-\frac{BFI^2}{4\varepsilon^2} p_i^2 \right) \left(\frac{\Delta k}{k_0} \right) \tag{10}$$

where *BFI* is the Benjamin-Feir index defined as (4). Thus, the number of discretization $ND = \Delta k / k_0$ is the main control parameter in the numerical experiment conducted here.

Typical evolution of discrete wave amplitudes in time is presented in Figure 6 (left) for *ND*=10. The spectral wave components included are in the range $0 < k < 2k_0$, so the total number of wave modes computed will be 20. Evolution is computed for 200 wave periods and the spectral shape averaged over the 200 wave periods is slightly distorted from the original (Figure 6 right). This is because the evolution becomes rather chaotic for a discrete wave system as first shown by Yuen and Lake (1982). The spikes that appear in the averaged spectrum seem to indicate the existence of the sideband instability or the Benjamin-Feir instability. The extreme event realized in this simulation is shown in Figure 7 left. The actual free surface shape is shown here including the bound wave effects (distortion of the wave shape). Overall, the wave height distribution does not agree with the Rayleigh distribution (Figure 7 right) and therefore the kurtosis becomes large. Next we systematically investigate the dependence of the number of discretization ND on the value of kurtosis for different BFI.

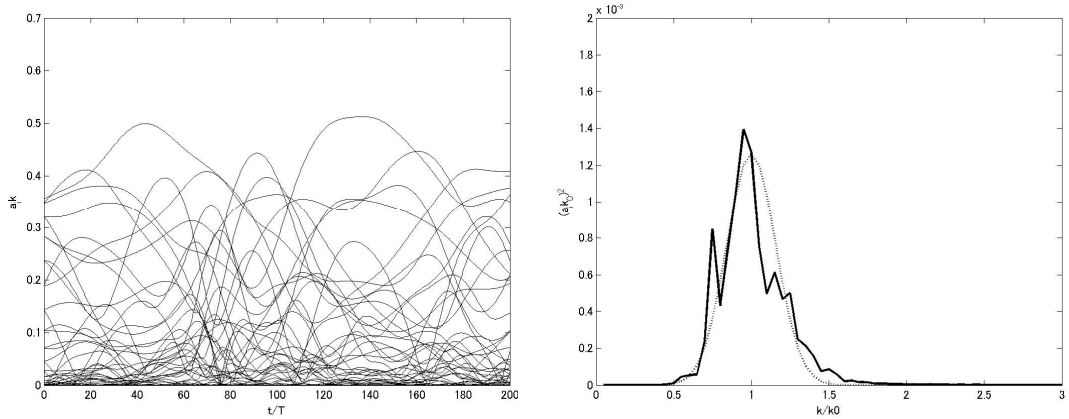

Figure 6: Left: Evolution of wave modes for 200 wave periods and ND=10 (total 20 wave modes). Right: Averaged wave amplitudes against wave number (thick solid line); narrow line indicates the initial spectral shape (Gaussian-bell shaped spectrum)

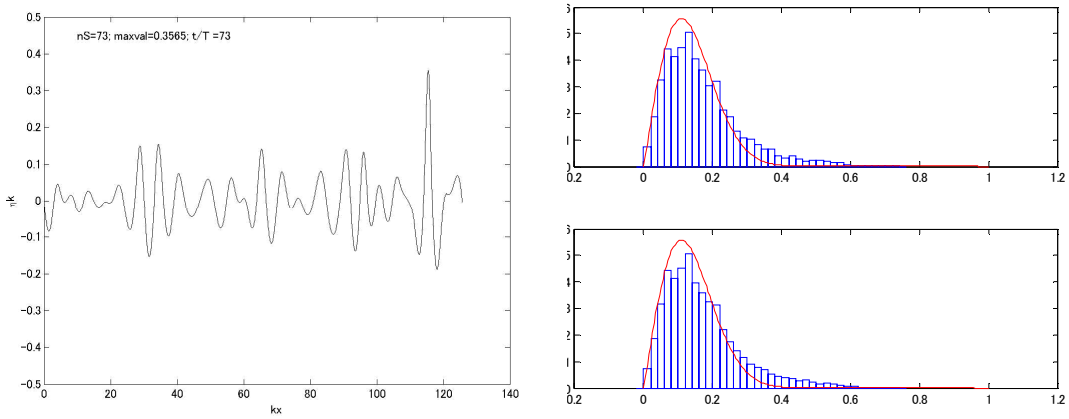

Figure 7: Left snap shot of surface elevation when maximum wave height is observed; Right: wave height histogram together with Rayleigh distribution (line), top zero-up-crossing, bottom zero-down-crossing.

The value of the kurtosis for a given parameter set is obtained by time averaging the kurtosis which changes quite a bit within 200 wave periods. Furthermore, since the averaged value depended on the selected random initial phase, we have conducted 10 ensemble runs for each parameter combination (BFI=0.2, 0.4, 0.6, 0.8, 1.0 and 1.2, ND=5, 10, 20, 40, 50, 80). In Figure 8, the mean kurtosis from the 10 ensemble runs (error bar one standard deviation) are plotted against number of discretization (ND) for different BFI. The estimated kurtosis tends to saturate rather rapidly from *ND*=20 and above. The result was somewhat surprising because the actual wave height distribution is quite different for low degrees of freedom system (ND<10, not shown). The result suggests that the value of kurtosis can be estimated numerically at relatively low degrees of freedom.

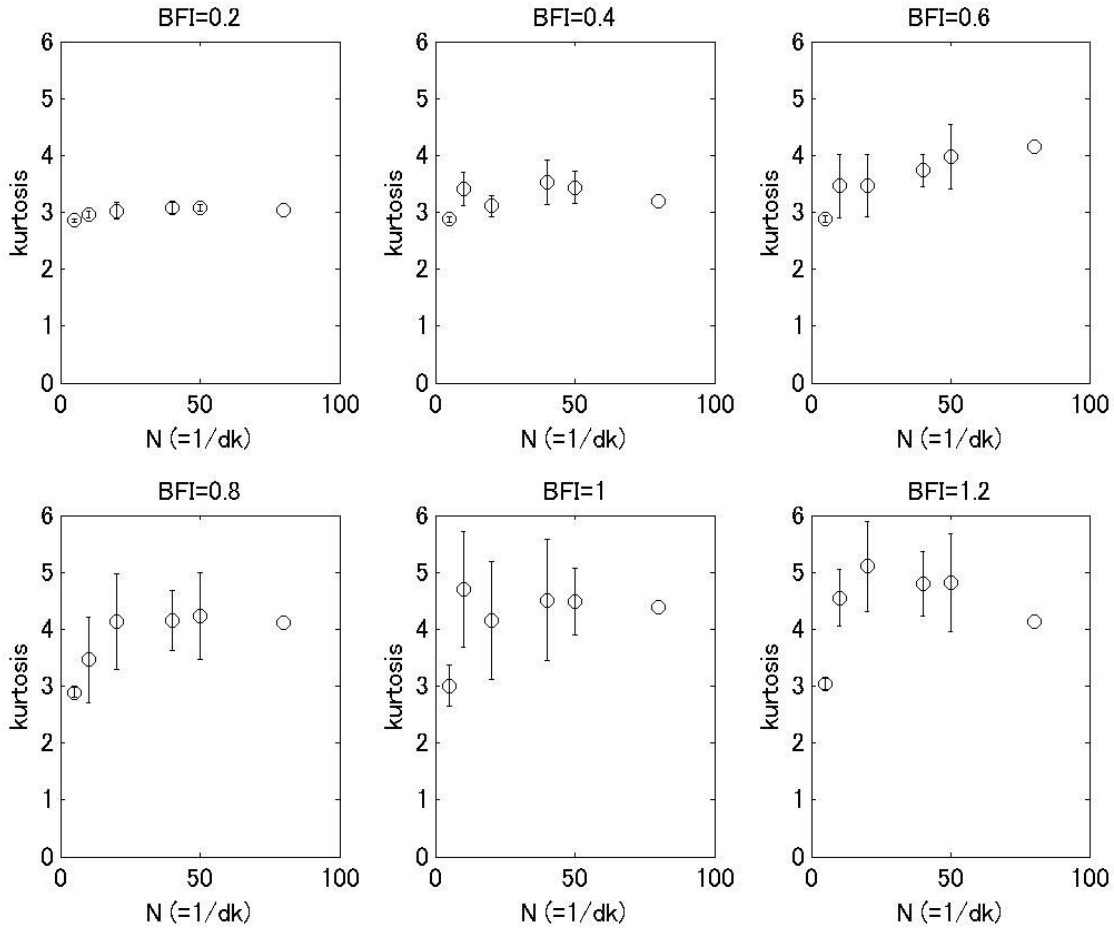

Figure 8: Kurtosis as a function of discretization level for different BFI. Mean and standard deviation is from 10 ensemble runs.

5. Conclusions

From the wave tank experiment impact of directionality on wave statistics were discussed:

1) For a given BFI (ε and δf/f) the magnitude of the Kurtosis significantly reduces as the directional spectra broadens
2) The extreme wave (Hmax>2.0 Hs) probability might still be related to the magnitude of the Kurtosis but the result is not conclusive yet
3) The BFI alone is not sufficient to model the Kurtosis of the directional wave and the theory needs to be extended to include directionality

From the numerical study impact of discreteness was discussed:

4) The magnitude of the Kurtosis significantly increases with higher degrees of freedom and seems to equilibrate
5) The magnitude of the Kurtosis might still be represented by a discrete wave system of relatively low degrees of freedom
6) Numerical simulation is useful in elucidating the effect of bound components and free waves but lacks the inclusion of breaking wave

Acknowledgement

The author thanks Drs. Kinoshita and Rheem for their help in conducting the tank experiment. The numerical solver of the Zhakarov equation was originally developed by O. Oshri in collaboration with T. Waseda at the U. of California Santa Barbara. The work was conducted as part of the grant-in-aid for scientific research (A) of the Japan Society for the Promotion of Science (JSPS).

6. References

Benjamin, T.B. and J.E. Feir, 1967, The disintegration of wave trains on deep water Part 1. Theory, J. Fluid Mech. 27, 417-

Dysthe, K. H. Socquet-Juglard, K. Trulsen, H. Krogstad, and J. Liu, "Freak" waves and large-scale simulations of surface gravity waves, Rogue Waves 2004, edited by M. Olagnon and M. Prevosto

Forristall, G., 1978, On the statistical distribution of waves heights in a storm, J. Geophys. Res., C5, 83, 2353-2358

Janssen, P.A.E.M., 2003, Nonlinear four-wave interactions and freak waves, J. Phys. Oceanogr., 33, 863-884

Krasitskii, V.P., 1994, On reduced equations in the Hamiltonian theory of weakly nonlinear surface waves, J. Fluid Mech., 272, 1-20

Melville, K., 1982, The instability and breaking of deep-water wave, J. Fluid Mech., 115, 165-185

Onorato, M., Osborne, A.R. and M. Serio, 2002, Extreme wave events in directional, random oceanic sea states, Physics of Fluids, 14 (4), 25-28

Onorato, M., A.R. Osborne, M. Serio, L. Cavaleri, C. Brandini, C.T. Stansberg, 2004, Observation of strongly non-Gaussian statistics for random sea surface gravity waves in wave flume experiments, Phys. Review E, 70, 067302

Onorato, M., Osborne, A.R. and M. Serio, 2005, On deviations from Gaussian statistics for surface gravity waves, preprint

Soquet-Juglard, H., K. Dysthe, K. Trulsen, H.E. Krogstat, J. Liu, 2005, Probability distribution of surface gravity waves during spectral changes, J. Fluid Mech., 542, 195-216

Yuen, H., and B. Lake, 1982, Nonlinear dynamics of deep-water gravity waves, Adv. Appl. Mech., 22, 67-229

Tulin, M.P. and T. Waseda, 1999, Laboratory observations of wave group evolution, including breaking effects, J. Fluid Mech., 378, 197-

Zakharov, V., 1968, Stability of periodic waves of finite amplitude on the surface of deep fluid, J. Appl. Mech. Tech. Phys. (English transl.), 2, 190-194